Eur. Phys. J. D **24**, 119–122 (2003)
DOI: 10.1140/epjd/e2003-00112-y

THE EUROPEAN PHYSICAL JOURNAL D

Temperature dependence of photoluminescence from mono-dispersed Si nanoparticles

T. Orii[1,a], M. Hirasawa[1], T. Seto[1], N. Aya[1], and S. Onari[2]

[1] Research Center for Advanced Manufacturing on Nanoscale Science and Engineering, National Institute of Advanced Industrial Science and Technology (AIST), 1-2-1 Namiki, Tsukuba, Ibaraki 305-8564, Japan
[2] Institute of Materials Science, University of Tsukuba, Tsukuba, Ibaraki 305-8573, Japan

Received 10 September 2002
Published online 3 July 2003 – © EDP Sciences, Società Italiana di Fisica, Springer-Verlag 2003

Abstract. The temperature dependence of photoluminescence (PL) from mono-dispersed Si nanoparticles was studied from 4 to 300 K. Si nanoparticles produced by pulsed laser ablation in He background gas were sorted into the 6 nm size range by a differential mobility analyzer (DMA). The spread of the size distribution was narrowed to a geometrical standard deviation $\sigma_g = 1.05$. On decreasing the temperature from 300 to 4 K, the intensity of the PL spectra increased gradually, peaked at about 60 K, and then decreased rapidly. The temperature dependences of the intensity and the full width at half maximum (FWHM) on the PL spectra are discussed in terms of radiative and nonradiative decay rates.

PACS. 61.46.+w Nanoscale materials: clusters, nanoparticules, nanotubes, and nanocrystals – 78.55.Ap Elemental semiconductors – 81.07.Bc Nanocrystalline materials

1 Introduction

Since strong visible light emission was first observed from porous Si [1], a great number of studies on the light emission from Si based nanostructures have been reported [2–10]. A quantum size effect of electron-hole pairs was proposed as one of the origins of the light emission at room temperature [1]. The temperature dependence of photoluminescence (PL) has been studied on porous Si [11] and Si nanoparticles [5,10], but the behavior was complicated. To explain the anomalous temperature dependence, Kanemitsu *et al.* proposed a three-region model [5] and Brongersma *et al.* applied a model premised on the energy splitting of singlet and triplet excitonic states by exchange interaction [9,10]. In the case of porous Si, the possibility of luminescent species existing at the surface [2,3], such as siloxene [2], which is produced in the anodization of Si wafers in HF based solution, have complicated the proof of the quantum size effect. In addition, broad size distributions of Si nanostructures have kept the origins of the light emission obscure.

The latest development of measurement systems enables one to observe PL spectra from single Si quantum dots [12,13]. Valenta *et al.* reported that the minimum FWHM of Gaussian profiled PL spectra from single Si nanopillars covered with SiO_2 was 0.12 eV at room temperature, though the size was not determined by direct measurement [12]. Korgel's group produced Si nanoparticles covered with organic molecules and observed size dependent PL spectra whose peaks ranged from red to blue [13,14]. The size dependence of the PL energy seems to be similar to that of the porous Si rather than that of Si nanoparticles covered with SiO_2 [6,9]. They reported that PL spectra was influenced by surface chemistry, especially oxidization, even if the surface was stabilized by organic molecules.

In this paper, we report the temperature dependence of PL spectra from Si nanoparticles produced by pulsed laser ablation (PLA) in an inert gas atmosphere. PLA has been employed as a synthetic method for Si nanoparticles [7] because PLA is one of the low contamination methods that produce nanoparticles of high melting point materials. Recently, the differential mobility analyzer (DMA), which had been used to select the size of aerosol particles at the atmospheric pressure, was improved to work for nanoparticles under low-pressure conditions [15]. By using a system where the PLA and DMA are combined [16], one can obtain mono-dispersed high purity Si nanoparticles that are suitable for investigation of the quantum size effect on photoluminescence. In our work, the Si nanoparticles are produced by the PLA and those with a diameter of 6 nm selected by DMA with a standard geometrical deviation of about 1.05. The temperature dependences of the intensity and the full width at half maximum (FWHM) of PL spectra from the mono-dispersed Si nanoparticles are discussed in terms of the quantum size effect.

[a] e-mail: t.orii@aist.go.jp

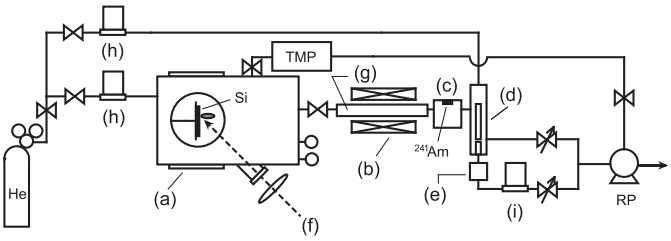

Fig. 1. Schematic view of the experimental setup: (a) ablation chamber, (b) electric furnace, (c) ionizer, (d) DMA, (e) deposition chamber, (f) SHG of Nd:YAG laser, (g) quartz tube, (h) mass flow controller, and (i) mass flow meter.

2 Experimental

A schematic diagram of the experimental setup is shown in Figure 1. The apparatus is composed of (a) an ablation chamber, (b) an electric furnace, (c) an ionizer, (d) the differential mobility analyzer (DMA) and (e) a deposition chamber [17]. The (f) second-harmonic Nd:YAG laser beam (532 nm line, pulse energy: 210 mJ, repetition rate: 10 Hz) was focused on the surface of a Si single crystal ((100) oriented p-type silicon wafer) in a He gas atmosphere (gas pressure: 7 torr). The Si nanoparticles formed in the ablation chamber were transferred with the He gas flow (flow rate: 400 sccm) and passed through (g) a quartz glass tube heated to 900 °C by the electric furnace for a post annealing process (PAP). The PAP acted to crystallize coalescent species of primary particles, such as clusters present in the He gas flow, and prevented them from interfering with the size-selection process of the DMA [17]. The DMA analyzes mobility depending upon the size of a charged particle in a laminar gas flow where an electrostatic potential is applied. Therefore, by changing the electrostatic potential applied to the DMA we can select a certain size of nanoparticle. A geometric particle size was evaluated by transmission electron microscopy (TEM) observation. The size-selected Si nanoparticles were deposited either on electron microscopic grids for TEM observation or on Ge wafer substrates for PL measurements.

PL spectra of Si nanoparticle deposition films were measured in a He gas ambient at temperatures ranging from 4 to 300 K by using a continuous flow He cryostat. The Si nanoparticle deposition film was irradiated by the 514.5 nm line of an argon-ion laser and the excitation power was kept at 250 mW/cm^2. PL spectra were measured using a single polychromator system equipped with a charge coupled device (CCD) detector cooled with liquid nitrogen. Scattered laser light from samples was eliminated by a holographic notch filter installed in front of the incident slit of the polychromator.

3 Results and discussion

Figure 2 show TEM image (Fig. 2a) and size distribution (Fig. 2b) of the Si nanoparticle sorted into the 6 nm size range by the DMA. Although many coalescent species had been observed without using PAP, by applying the post annealing at 900 °C, only spherical Si nanoparticles were observed, as shown in Figure 2a. As shown Figure 2b, the size distribution was very narrow and could be fitted successfully with a lognormal function. The average size was 6.9 nm and the geometrical standard deviation σ_g was 1.05. This value of σ_g corresponds to FWHM of about 0.8 nm. The average size (6.9 nm) estimated by the TEM observation was significantly larger than the nominal size (6.0 nm) which was the set point of size-selection by the DMA. According to a high-resolution TEM observation, the Si nanoparticles exhibited a core-shell structure. The core was a single crystalline structure whose lattice constant coincided with the bulk Si crystal. The shell was an amorphous structure and considered to be silicon oxide, since the sample was exposed to the atmosphere during transportation. The increase in the average size observed by the TEM is most likely caused by the formation of SiO_2 shell after the size-selection. The width of the shell was estimated to be 1.0 nm. The size distribution, shown in Figure 2b, corresponds to the outer diameter of the core-shell structure; therefore, the Si crystalline domain size in nanoparticle was estimated to approximately 4.9 nm.

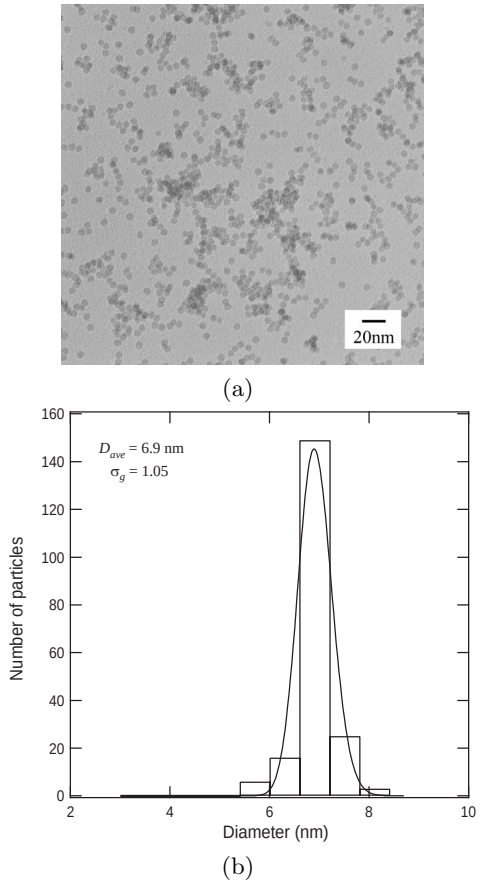

Fig. 2. (a) TEM image of mono-dispersed Si nanoparticles whose size was selected at 6 nm by DMA. (b) Size distribution of Si nanoparticles. The solid curve represents the best fit to the data using a lognormal function whose peak size is 6.9 nm and a geometrical standard deviation σ_g is equal to 1.05. This σ_g corresponds to a FWHM of 0.8 nm.

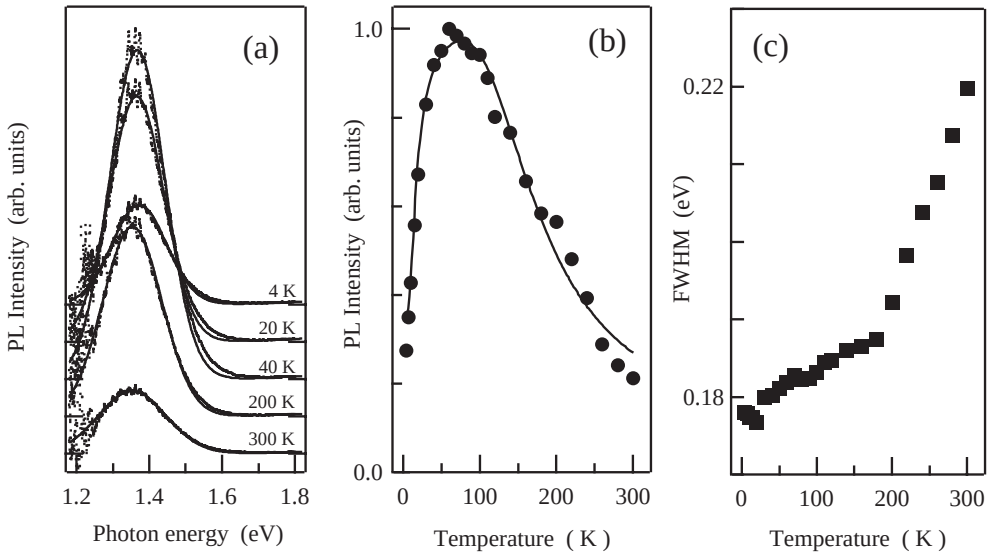

Fig. 3. (a) PL spectra of mono-dispersed Si nanoparticles measured at temperatures of 4, 20, 40, 200, and 300 K. The solid lines represent the best fit to the data using a Gaussian function. (b) Temperature dependence of PL intensity. The solid lines represent the best fit to the data using a theoretical quantum efficiency. (c) Temperature dependence of the FWHM.

Figure 3a shows the PL spectra of the mono-dispersed Si nanoparticle measured at 4, 20, 40, 200 and 300 K. A sharp PL spectrum was observed in the near-infrared region at room temperature. At 300 K, the peak energy was 1.35 eV, higher than the band-gap energy of bulk Si by 0.23 eV. This PL energy was not noticeably different from that of Si nanoparticles reported previously [8,9]. As shown in Figure 3a, this PL spectrum was fitted successfully with a Gaussian function. In general, a broad size distribution brings extrinsic width to PL spectra of nanoparticles. In this work, the size-selection by DMA narrowed the FWHM of the PL spectrum from a Si nanoparticle deposition film to 0.22 eV at room temperature.

On decreasing the temperature from 300 to 4 K, the intensity of the PL spectra increased gradually, peaked at about 60 K and then decreased rapidly. The integrated intensity of the PL spectra was plotted as a function of the temperature ranging between 300 and 4 K in Figure 3b. The PL intensity at 60 K was increased relative to the value at 300 K by a factor of 5 and that at 4 K decreased roughly to the value at 300 K. This complicated temperature dependence of PL intensity can be explained by considering a temperature dependent radiative decay rate R_r and a nonradiative decay rate R_n. The PL intensity $I_{PL}(T)$ is in proportional to the quantum efficiency, therefore,

$$I_{PL}(T) \propto R_r/(R_r + R_n). \tag{1}$$

Now, we do not have any information about R_r for our sample. However, the splitting model of luminescent states proposed by Calcott *et al.* for porous Si [4] give us a useful expression for the temperature dependent radiative decay rate. According to this model, the luminescent excitonic states are split to a singlet state and a triplet state with a splitting energy ΔE due to the exchange interaction. At very low temperatures, almost all of the excitons are trapped in the lower triplet state. With temperature some of them are excited to the upper singlet state which is a dominant luminescent center and R_r is given by

$$R_r = \frac{3R_t + R_s \exp(-\Delta E/k_B T)}{3 + \exp(-\Delta E/k_B T)}, \tag{2}$$

where R_s and R_t are radiative decay rates of the singlet state and of the triplet state, respectively. Next, we assumed that R_n was composed of a thermally activated process and a nonthermal process, so that

$$R_n = \eta f_0 \exp(-E_a/k_B T) + R'_n, \tag{3}$$

where η, f_0, E_a and R'_n are the transition efficiency, the attempt frequency, activation energy and nonthermal factor, respectively. We tried fitting the temperature dependence of the PL intensity by substituting equations (2, 3) for equation (1). In the fitting, the values of R_s, R_t and f_0 were fixed to 8500, 150 s^{-1} [9] and 10^{12} s^{-1} [8]. The best of least squares fit results shown in Figure 3b with a solid curve, which reproduces successfully the temperature dependence of PL intensity. The best set of fitting parameters is found to be $\Delta E = 3.4$ meV, $\eta = 5.0 \times 10^{-8}$, $E_a = 52$ meV and $R'_n = 373\ s^{-1}$. The splitting energy ΔE agrees very well with the values estimated by means of a time-resolved PL measurement [9,10]. On the other hand, the value of η seems to be extremely small.

First, we discuss the temperature dependence of the PL intensity at temperatures lower than 60 K. In this low temperature region, the decrease of PL intensity with decreasing temperature was not reproduced by the fitting when the nonthermal factor R'_n was removed from equation (3), because the thermally activated process became negligible. The rate of the nonthermal process R'_n is approximately twice as large as R_t and is the dominant decay rate at temperatures lower than about 40 K. Therefore, the nonthermal process increases its importance and influences the quantum efficiency. Suemoto *et al.* assigned the nonthermal process to a tunneling escape of carriers through barrier potential of shell [18].

In the region of temperature higher than 60 K, the thermally activated process becomes predominant and

is the main in reducing the quantum efficiency with an increase in temperature. In Figure 3c, we plotted the FWHM of PL spectra as a function of temperature. The FWHM decreased with decreasing temperature from 300 to 40 K and the temperature dependence exhibited a sharp bend at 180 K, in spite of the fact that the PL intensity did not show so obvious a change at that temperature. The line width of the PL peak generally correlates with the lifetime and the distribution of carriers. An increase in the radiative lifetime R_r with a decrease of temperature have been reported for Si nanoparticles surrounded with SiO_2 [9,10] and corresponds to a narrowing of the line width. However, the bending cannot be explained only with the temperature dependence of R_r. English *et al.* reported that the decay mechanism of excitons in the Si nanoparticle covered with organic molecules was affected with oxygen-related surface states which can trap excitons [13]. For Si nanoparticles covered with amorphous SiO_2, another thermally activated process, *e.g.* nonradiative recombination at Si/SiO_2 interface states, should be considered to explain our temperature dependence of line width. Below 40 K, the FWHM did not decrease but actually increased slightly at temperature below 20 K, although the radiative lifetime increases drastically in this temperature range. This temperature dependence at temperatures below 20 K is probably caused by a competition between the increase of the radiative lifetime and the thermal redistribution of carriers from the triplet state to the singlet state.

4 Summary

The temperature dependence of PL spectra from monodispersed Si nanoparticles whose average size was 6 nm was studied. On decreasing the temperature from 300 to 4 K, the intensity of the PL spectra increased gradually, peaked at about 60 K and then decreased rapidly. The temperature dependence of PL intensity was explained well by considering that the quantum efficiency is composed of a radiative decay rate premised on the splitting model of luminescent states and a nonradiative decay rate premised on thermally activated and nonthermal processes. The nonthermal process causes the decrease of PL intensity at temperatures lower than 60 K.

This work was partially sponsored by the Advanced Photon Manufacturing and Measurement Technology Project with support from METI and the New Energy and Industrial Technology Development Organization (NEDO).

References

1. L.T. Canhan. Appl. Phys. Lett. **57**, 1046 (1990)
2. M.S. Brandt, H.D. Fuchs, M. Stutzmann, J. Weber, M. Cardona, Solid State Commun. **81**, 307 (1992)
3. R.P. Vasquez, R.W. Fathauer, T. George, A. Ksendzov, T.L. Lin, Appl. Phys. Lett. **60**, 1004 (1992)
4. P.D.J. Calcott, K.J. Nash, L.T. Canham, M.J. Kane, D. Brumhead, J. Phys. Cond. Matt. **5**, L91 (1993)
5. Y. Kanemitsu, T. Ogawa, K. Shiraishi, K. Takeda, Phys. Rev. B **48**, 4883 (1993)
6. S. Schuppler, S.L. Friedman, M.A. Marcus, D.L. Adler, Y.-H. Xie, F.M. Ross, Y.J. Chabal, T.D. Harris, L.E. Brus, W.L. Brown, E.E. Chaban, P.F. Szajowski, S.B. Christman, P.H. Citrin, Phys. Rev. B **52**, 4910 (1995)
7. Y. Yamada, T. Orii, I. Umezu, S. Takeyama, T. Yoshida, Jpn J. Appl. Phys. **35**, 1361 (1996)
8. M. Ehbrecht, B. Kohn, F, Huisken, M.A. Lagun, V. Paillard, Phys. Rev. B **56**, 6958 (1997)
9. S. Takeoka, M. Fujii, S. Hayashi, Phys. Rev. B **62**, 16820 (2000)
10. M.L. Brongersma, P.G. Kik, A. Polman, K.S. Min, H.A. Atwater, Appl. Phys. Lett. **76**, 351 (2000)
11. Y. Kanemitsu, H. Uto, Y. Masumoto, T. Matsumoto, T. Futagi, H. Miura, Phys. Rev. B **48**, 2827 (1993)
12. J. Valenta, R. Juhasz, J. Linnros, J. Lumin. **98**, 15 (2002)
13. D.S. English, L.E. Pell, Z. Yu, P.F. Barbara, B.A. Korgel, Nano Lett. **2**, 681 (2002)
14. J.D. Holmes, K.J. Ziegler, R.C. Doty, L.E. Pell, K.P. Johnston, B.A. Korgel, J. Am. Chem. Soc. **123**, 3743 (2001)
15. T. Seto, T. Nakamoto, K. Okuyama, M. Adachi, Y. Kuga, K Takeuchi, J. Aerosol Sci. **28**, 193 (1997)
16. N. Suzuki, T. Makino, Y. Yamada, T. Yoshida, T. Seto, Appl. Phys. Lett. **78**, 2043 (2001)
17. M. Hirasawa, T. Seto, N. Aya, J. Nanosci. Nanotech. **1**, 381 (2001)
18. T. Suemoto, K. Tanaka, A. Nakajima, Phys. Rev. B **49**, 11005 (1994)